Atmospheric Environment 141 (2016) 96–105

Contents lists available at ScienceDirect

Atmospheric Environment

journal homepage: www.elsevier.com/locate/atmosenv

Flux estimation of fugitive particulate matter emissions from loose Calcisols at construction sites

Hala A. Hassan [a, b], Prashant Kumar [b, c], Konstantinos E. Kakosimos [a, *]

[a] Department of Chemical Engineering, Texas A&M University at Qatar, 23874 Doha, Qatar
[b] Department of Civil and Environmental Engineering, Faculty of Engineering and Physical Sciences, University of Surrey, Guildford GU2 7XH, United Kingdom
[c] Environmental Flow (EnFlo) Research Centre, Faculty of Engineering and Physical Sciences, University of Surrey, Guildford GU2 7XH, United Kingdom

HIGHLIGHTS

- Fugitive PM (fPM) emissions due to wind erosion at construction sites were assessed.
- Field measurements and modeling for the estimation of fPM emissions carried out.
- Emission flux functions developed for four particle size classes of loose Calcisols.
- Good agreement found between modeled and measured concentrations.
- High uncertainty was observed for both developed and literature flux functions.

ARTICLE INFO

Article history:
Received 21 October 2015
Received in revised form
20 June 2016
Accepted 21 June 2016
Available online 22 June 2016

Keywords:
Air pollution
Construction emissions
Fugitive particulate matter
Carbonates
Calcisols
Middle-east region

ABSTRACT

A major source of airborne pollution in arid and semi-arid environments (i.e. North Africa, Middle East, Central Asia, and Australia) is the fugitive particulate matter (fPM), which is a frequent product of wind erosion. However, accurate determination of fPM is an ongoing scientific challenge. The objective of this study is to examine fPM emissions from the loose Calcisols (i.e. soils with a substantial accumulation of secondary carbonates), owing to construction activities that can be frequently seen nowadays in arid urbanizing regions such as the Middle East. A two months field campaign was conducted at a construction site, at rest, within the city of Doha (Qatar) to measure number concentrations of PM over a size range of 0.25–32 μm using light scattering based monitoring stations. The fPM emission fluxes were calculated using the Fugitive Dust Model (FDM) in an iterative manner and were fitted to a power function, which expresses the wind velocity dependence. The power factors were estimated as 1.87, 1.65, 2.70 and 2.06 for the four different size classes of particles ≤2.5, 2.5–6, 6–10 and ≤10 μm, respectively. Fitted power function was considered acceptable given that adjusted R^2 values varied from 0.13 for the smaller particles and up to 0.69 for the larger ones. These power factors are in the same range of those reported in the literature for similar sources. The outcome of this study is expected to contribute to the improvement of PM emission inventories by focusing on an overlooked but significant pollution source, especially in dry and arid regions, and often located very close to residential areas and sensitive population groups. Further campaigns are recommended to reduce the uncertainty and include more fPM sources (e.g. earthworks) and other types of soil.

1. Introduction

A major source of airborne pollution in dry arid lands is the fugitive particulate matter (fPM), which is a frequent product of soil erosion from winds (Tsiouri et al., 2014). The meteorology and low vegetation cover of arid regions make them highly susceptible to wind-blown particles. On the other hand, many such regions, like the Middle East Area (MEA), are experiencing rapid rates of urbanization, industrialization and construction, resulting in increased human exposure to the airborne PM. Significant emissions of PM in these areas come from industry, construction, road

* Corresponding author.
E-mail address: kkakosim@gmail.com (K.E. Kakosimos).

http://dx.doi.org/10.1016/j.atmosenv.2016.06.054
1352-2310/

traffic and natural sources (Tsiouri et al., 2014). Studies in Kuwait, Iraq and Iran have reported hazardous minerals associated with the transported dust (Bu-Olayan and Thomas, 2012; Engelbrecht and Jayanty, 2013; Rashki et al., 2013). The World Health Organization (WHO) had set annual mean limits for PM_{10} (i.e. ≤10 μm in aerodynamic diameter) and $PM_{2.5}$ (i.e. ≤2.5 μm) of 20 μg m^{-3} and 10 μg m^{-3}, respectively (WHO, 2005). However, PM levels exceeding 6–8 times the WHO guidelines were recently observed in many cities in the arid Middle Eastern region (WHO, 2014). For example, PM_{10} annual mean concentrations have been reported as 128 μg m^{-3} in Amman, 135 μg m^{-3} in Cairo, 168 μg m^{-3} Doha, and 170 μg m^{-3} in Abu Dhabi between the years 2010 and 2012 (WHO, 2014). There are substantial evidence that airborne PM contributes to haze, acid rain, global climate change, asthma, cardiopulmonary disease and decreased life expectancy (Heal et al., 2012; Kumar et al., 2014). The severity of health effects due to PM exposure depends mainly on the levels of ambient concentration and the length of exposure (Pope III and Dockery, 2006). This is evident from the link between ambient PM pollution and increased mortality through several studies over the past decade (Chen and Lippmann, 2009; Pope III and Dockery, 2006; Samoli et al., 2008). Although chemically "inert" and just a portion of airborne particles, fPM cannot be ignored as they comprise the majority of PM in many arid and semi-arid environments (Marticorena and Bergametti, 1995) and need to be studied and regulated (USEPA, 2011).

According to the Food and Agriculture Organization (FAO, 2014), one of the most common reference soil groups of arid and semi-arid environments are the Calcisols, formerly been called "Desert Soils". These soils cover big areas of Middle-East, North Africa, Central Asia and Australia (see Fig. 1). Emission inventories for dust particles and PM are available for European (EMEP/EEA, 2013) and North American (EMEP/EEA, 2013; USEPA, 1995) domains. These inventories cover information on fugitive emissions from some sources such as agricultural (Pouliot et al., 2012), while non-exhaust vehicle emissions and emissions produced by wind shear and material transfer processes remain poorly attended (Kumar et al., 2013; Winiwarter et al., 2009) and limited to the regional scale (Schaap et al., 2009).

Determination of fPM emissions has been an ongoing challenge for the air quality research community because of the induced health effects and the large uncertainty in their determination (Neuman et al., 2009; Roney and White, 2006). Different approaches such as field measurements (Brown et al., 1995; Kouyoumdjian and Saliba, 2006; Shahsavani et al., 2012), laboratory scale testing (Neuman et al., 2009; Roney and White, 2006) and dispersion modeling (Ono et al., 2011) have been used for developing adequate techniques to estimate fPM emissions. In the work of Ono (2006), sand flux measurements from four areas at Owens Lake, California (USA) were measured using low-cost Cox Sand Catchers (CSC) and electronic sensors. These measurements were used to empirically determine the surface erosion potential, followed by an application of Gillette Model to estimate the sand flux. The latter provided good predictions (R^2 ranging from 0.72 to 0.87) when compared to the measured hourly sand flux rates. Recently, Ono et al. (2011) quantified the windblown PM_{10} from Mono Lake in California (USA), using the Dust Identification (Dust ID) method. In this method, PM_{10} emissions are calculated using the proportionality ratio (presented as K-factor) between the vertical and horizontal flux of PM_{10}; these fluxes are estimated using the mass of saltating particles measured by CSCs. Hourly emissions were then entered into a dispersion model (AERMOD – American Meteorological Society/Environmental Protection Agency Regulatory Model) to predict hourly PM_{10} concentrations. The model predictions were compared to the concentrations measured on-site in order to calculate hourly K-factors, and use them to re-calculate hourly PM_{10} emissions. This method, which accounts for the change in surface conditions, provided good results (factor of two, FAC2 = 60.2%, R^2 = 0.77 between modeled and observed data) compared to the wind tunnel-based emissions measured for the same surface. Kinsey et al. (2004) used time-integrated and continuous exposure profiling to evaluate the emission factors of PM_{10} and $PM_{2.5}$ for mud carry out from a major construction site in metropolitan Kansas City in Missouri (USA). Time-integrated air sampling was conducted using high-volume air samplers to collect PM_{10} and $PM_{2.5}$ samples from the site. In addition, vacuum sweeping was used to collect surface samples for the analysis of roadway material, and pneumatic traffic counters and visual recordings for the vehicle loads. Emission factors (expressed in mass

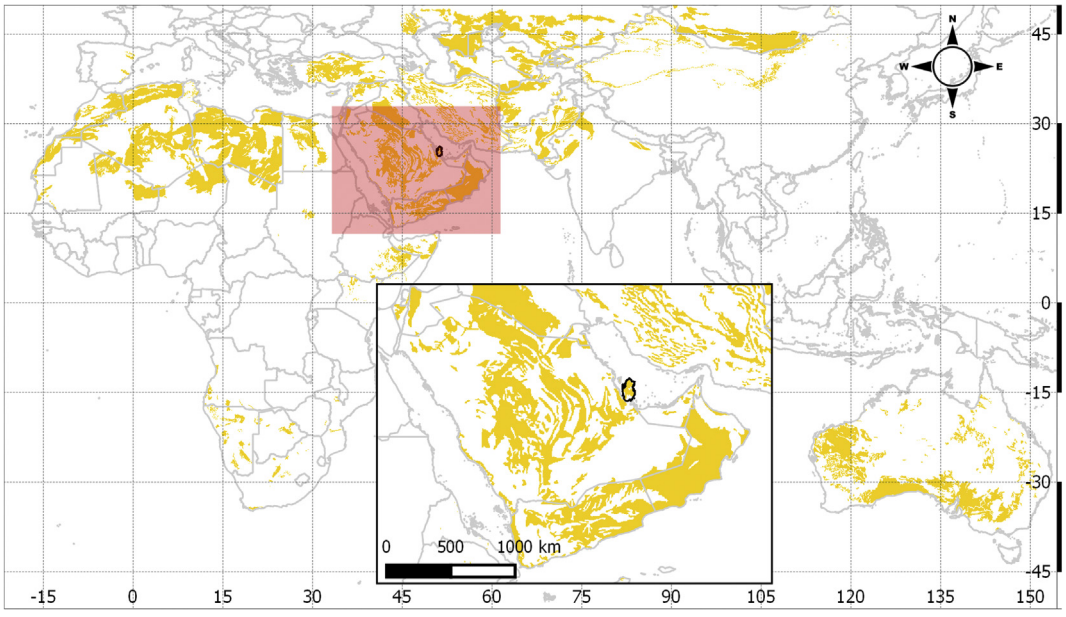

Fig. 1. Map showing main worldwide areas and the Middle East (inset) covered by Calcisols (FAO, 2014).

emitted per vehicle distance traveled, μg km^{-1}) were calculated by normalizing the spatially integrated exposure (total particle mass collected) against traffic volume (total distance traveled from all vehicles). The resulted PM_{10} emission factor was found to be within the range reported earlier (USEPA, 1995) but $PM_{2.5}$ factor was far lower. Another work was presented by Abdul-Wahab (2006) to assess the impact of fPM emissions from cement plant activities using the fugitive dust model (FDM). Her work made estimates of the emission rates using the empirical emission factors reported in the Australian National Pollutant Inventory (NPI, 1999), and entered them along with the meteorological and receptor data into the FDM to compute the dust emission concentrations. Model predictions were compared to the actual concentrations measured at residential areas adjacent to a cement plant. These measurements were measured using high volume samplers that collect total suspended particulates (TSP) and calculate their concentrations using the sample volume. Although the model showed an under-prediction of the measured concentrations, a correlation coefficient of ($R^2 = 0.92$) was obtained when comparing predicted and measured values.

Other studies followed the wind-tunnel approach, such as the work presented by Roney and White (2006), to determine fPM emissions from Owen's (dry) Lake in California (USA) using an environmental boundary layer wind tunnel (Saltation Wind Tunnel – SWT). The tunnel was used to measure PM_{10} concentrations and vertical velocity for multiple soil samples and different surface conditions. The emission rates were then obtained through a material balance of the control volume and the inlet/outlet mass fluxes. The ratios of vertical flux/horizontal flux and horizontal flux/total soil flux were calculated and plotted using the wind tunnel results and were found to agree with other field studies (Gillette et al., 1997; Niemeyer et al., 1999) of Owen's Lake. A similar wind-tunnel approach was followed by Neuman et al. (2009) to obtain the relationship between fPM emissions, wind velocity and water content of mine tailings. Recently, Sanderson et al. (2014) also found good agreement between wind tunnel and field measurements when applied to fugitive emission rates from a large nickel smelter in Sudbury, Ontario (Canada). In their work, mass emission rate was measured through a wind tunnel experiment using the control volume method while vertical dust flux was determined using finite difference approximation. A comparison showed a strong agreement between the measured rate and flux ($R^2 = 0.99$), and that both vary with friction velocity with a strong correlation ($R^2 = 0.80–0.95$). In the work of Yuwono et al. (2014), wind speed and soil moisture dependent emission factors were developed to calculate dustfall and suspended particles from two different types of soil (Oxisol and Ultisol). Dustfall and suspended particles were measured for a number of collected soil samples using a lab scale wind tunnel, followed by a statistical analysis to obtain the Pearson correlations and the relative contribution of wind speed and soil moisture, and their exponential relation to the dust generation rate.

For the air quality management, emission estimates are necessary in order to evaluate the sources, design control strategies and develop suitable mitigation techniques. One way to quantify emissions is using the empirical factors developed by well-established environmental institutions. However, information on fPM emissions in the currently available inventories is limited compared to a large number of different sources that can produce fPM emissions. Furthermore, using analogs factors may results in inaccuracies when applied to certain surfaces of interest (Sanderson et al., 2014). It is worth noting here that the existing factors were developed for certain geographical regions (e.g. geology) and weather conditions, which may lead to inaccuracies when applied to other conditions. Up to date, the vast majority of studies on fPM emissions modeling focus on the wind erosion of typical soils and bare lands of North America and Europe.

In this study, we focus on the fPM emissions modeling from a common soil – the Calcisols – in dry and semi-dry regions of North-Africa, Middle East, Central Asia and Australia (Fig. 1). In addition, we consider the wind erosion of loose soil owes to human activities i.e. construction earthworks. We employ both, the field measurements and dispersion modeling, to correlate meteorological variables, fPM concentrations, and emission fluxes. The overall objective is to understand the Aeolian erosion mechanisms and obtain the emission factors of fPM produced by a specific type of soil and surface conditions. Therefore, we chose a construction site at rest as a study area, located within the City of Doha, State of Qatar. To the best of our knowledge, this is a unique study focusing on fPM from construction areas, which are usually very close to, or within residential areas and has a direct impact on the local air quality.

2. Methodology

An experimental field campaign and dispersion modeling are combined in order to examine the relationship between the meteorological variables and fPM emissions, and develop the specific functions for the emission fluxes (i.e. emission rates per area). The field campaign was conducted for measuring number concentrations at two locations – a construction site and a background location. Thereafter we used a dispersion model – FDM (Winges, 1991) – in an iterative manner to estimate the source-receptor relationship. The modeling and experimental results were post-processed for the calculation of the emission fluxes and the development of their new functions. Finally, these functions were compared with the functions reported in USEPA's AP-42 (USEPA, 1995), and also applied for the calculation of ground level PM concentrations, as a step of evaluation.

2.1. Site description

The experimental field campaign was conducted for a period of two months between April and May 2014. Particle number concentrations and meteorological parameters (i.e. wind speed, wind direction, relative humidity, ambient pressure and temperature) were measured at two locations: a construction site (which is also the studied source) and a background location (Fig. 2a). The background station was placed on the rooftop of a building (height = 10 m) located ~1.5 km away (northeast) from the construction site station which was located at the southern boundary of the construction site (Fig. 2b). Both sites are located within the Education City of Doha, (State of Qatar); the Education city is a complex that hosts branch campuses of seven international universities, a number of research centers, industry-related offices and student recreational activities (Fig. 2a). In this complex, most buildings are of low height (1–2 floors; <10 m). Although there are some buildings with 3–4 floors, none of them is directly in between the two monitoring sites. On the other hand, there is a wide road in between the two sites with considerable traffic (both light and heavy duty vehicles), but still equivalent to all other surrounding roads. The specific construction site (~0.15 km^2; Fig. 2b) was selected because it was at rest during the campaign, so we consider that Aeolian erosion of the loose soil was the only source of fPM. The site was also chosen as it represents a typical open bare land covered by the carbonates based soil of the region, highly susceptible to wind activity and close to residential areas (Fig. 2a). According to the wind roses diagrams for the monitoring stations, no significant impact was observed from nearby buildings and obstacles on their wind velocity and direction (Fig. 3). We also studied a

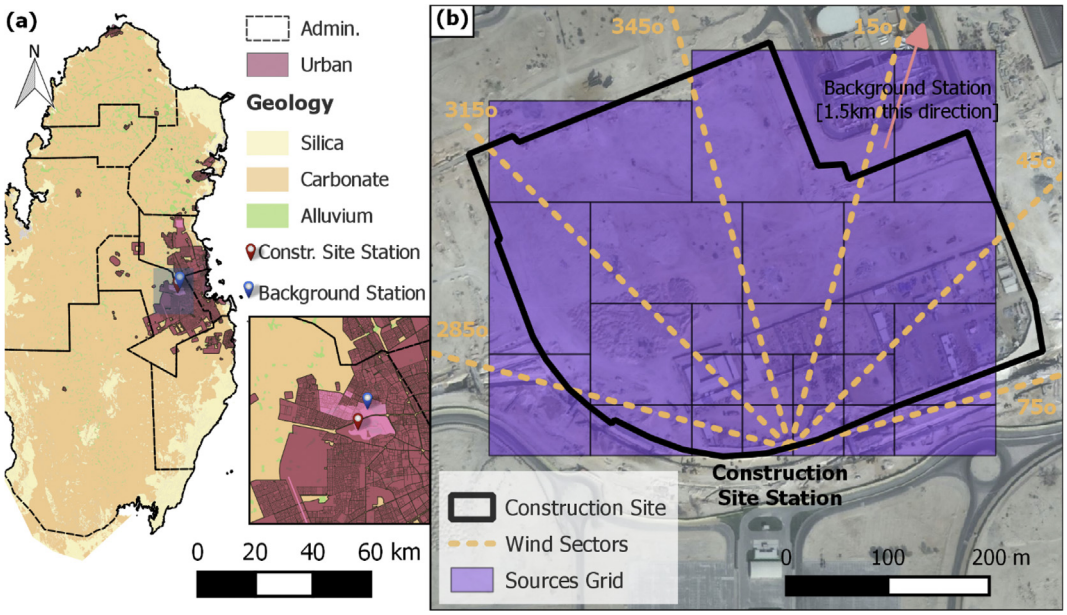

Fig. 2. The study area showing: (a) Qatar geological map and sites locations, (b) outline of the construction site and the formed 23 area sources (Section 2.3).

number of polar plots (Fig. 3b and c: mean PM_{10} concentrations and Fig. S1: weighted mean PM_{10} concentrations by wind speed/directions) and observed negligible influence by other major sources for the selected wind directions (i.e. WNW (West-northwest) to ENE (East-northeast)).

2.2. Data collection

PM number concentrations and meteorological data were collected using Environ Check 365#, which is an air quality monitoring station manufactured by Grimm Aerosol Technik GmbH & Co. KG, Germany (Grimm, 2009). The measurement method is based on laser light scattering. The monitoring station was used to measure both, particle number and mass concentrations, over a size range of 0.25 up to 32 μm in 31 size channels using a sampling rate of 1.2 lit min^{-1}. It produces particle mass concentrations [μg m^{-3}] using a proprietary algorithm calibrated to the National Institute of Standards and Technology (NIST, USA) Arizona test dust. According to vendor's certificate, measurements are equivalent to the European Standards EN12341 and EN14907. Prior to the field campaign, a side-by-side intercomparison was conducted between the two monitoring stations for two weeks, which resulted in standardized differences of less than 7% (i.e. the maximum of the distribution of the differences was in all cases within the uncertainty limits of the calibration standards ±3%).

The main input data required to run the FDM model include meteorological data, sources information, receptors information and particles characteristics. Meteorological measurements on a minute basis were recorded by the climate sensor (WS600-UMB by Luft, US) attached to the monitoring station. The accuracy of these measurements was ±0.2 °C for temperature (range −20–50 °C), ±2% for relative humidity (range 0–100%), ±0.3 m s^{-1} (response threshold 0.3 m s^{-1}) for wind speed, and ±3° (threshold 1 m s^{-1}) for wind direction.

Averaging of wind direction was computed by the Mitsuta method (Mori, 1986). In the absence of atmospheric stability measurements or output from the local meteorological agency, we obtained it using the turbulence-based (σ_A) method (USEPA, 2000). This method employs the standard deviation of wind direction and the scalar mean wind speed for the calculation of the hourly atmospheric stability. Previously (Gopalaswami et al., 2015), we have tested both the wind direction and stability methodologies in comparison with measurements and mesoscale model calculations, respectively, with good agreement. Mixing heights were also required by the model as part of the meteorological inputs. General values of the mixing height (from 400 m to 1800 m) were assigned for each time period following a stability class based approach (Winges, 1991). This assumption was considered adequate because of the small size of the site and the vicinity of the monitoring station to the emission sources. Finally, a roughness length of around 0.06 cm was selected following the textbook guidelines, which corresponds to a flat desert terrain. This assumption is considered valid for the internal boundary layer where both the source and monitoring station are located (Barlow, 2014).

2.3. Atmospheric dispersion modeling

The United States Environmental Protection Agency (USEPA) has approved a wide range of well-validated atmospheric dispersion models that can predict concentrations of various air pollutants on both local and regional scales (USEPA, 2005). Most of these models are either limited to gaseous pollutants or designed for large spatial domains. In addition, lack of specific modules to treat different particle sizes may induce deviations on the estimation of concentrations from fugitive dust emission sources (Abdul-Wahab, 2006). In this study, we aimed to choose a simpler model in order to facilitate inverse calculations.

The FDM, which is selected in this study, is a USEPA developed air quality model designed specifically to compute emissions and deposition impacts of fugitive dust sources (Winges, 1991). Although this model is no longer available on the USEPA's website (last version 1993), it has been used in the latter years by researchers and showed satisfactory results in predicting fPM from different industrial (e.g. cement and coal mines) sources (Abdul-Wahab, 2006; Trivedi et al., 2009). A study by Prabha (2006) showed a comparison between FDM and the Industrial Source Complex Short Term Model (ISCST3) for the short-term simulated emissions from mining activities. The FDM model showed a high

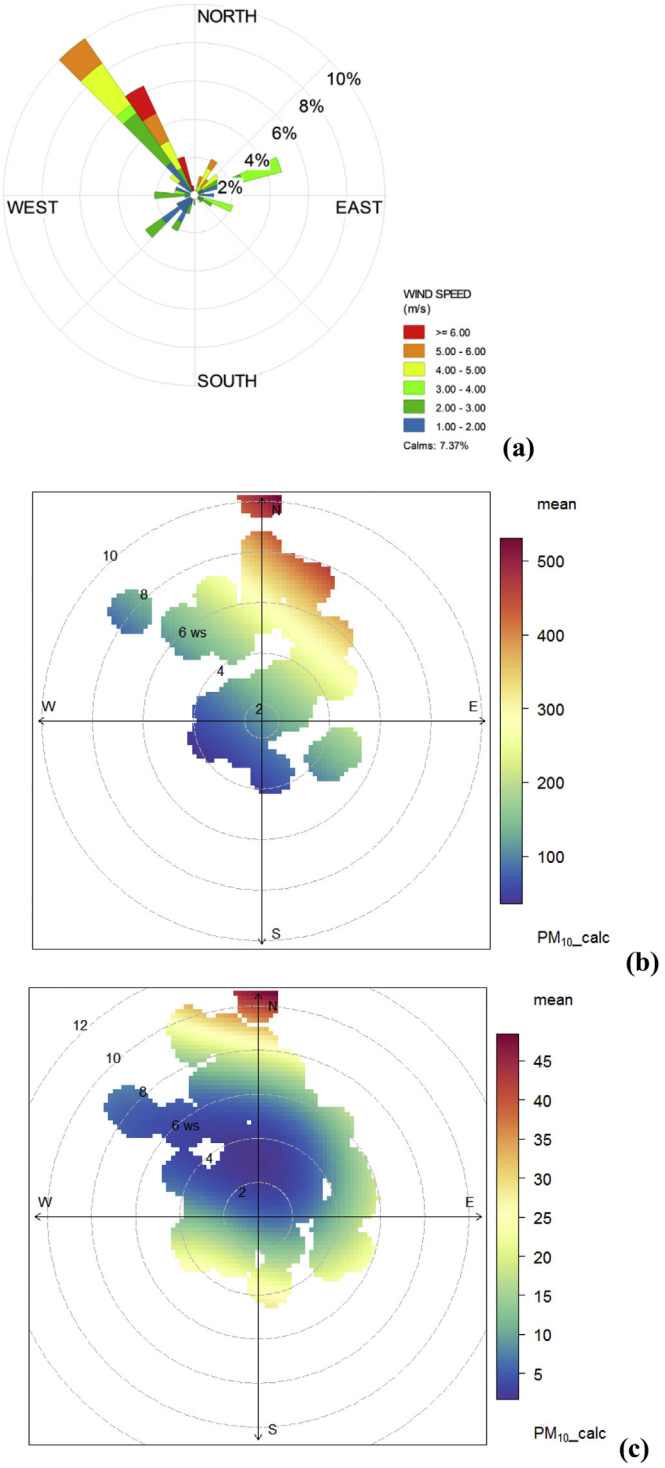

Fig. 3. (a) Wind rose for the construction site station during the studied period. Polar plots of PM_{10} mean concentration (μg m^{-3}) by wind speed (m s^{-1}), (b) for the construction site station during the study period, and (c) for the background station during the study period.

accuracy (d = 82%; index of agreement) in predicting emissions compared ISCST3 model (d = 44%). Another comparison is presented in Scott and Proctor (2008), verifying the significance of vehicle traffic and wind-eroded TSP (from chromite ore processing residue affected soils) and their associated inhalation risks. Using three different dispersion models (FDM, ISCST3, and AERMOD), emission estimates within an FAC2 were achieved by both (FDM) and (ISCST3) while the values predicted by AERMOD were as much as 5-folds of the measured.

FDM is based on the Gaussian plume formulation but specifically adapted to incorporate an improved gradient-transfer deposition algorithm. Emissions of each source are split into a number of particle size classes, where a gravitational settling velocity and a deposition velocity are computed by the model for each class. The pollutant transport is ruled by the general atmospheric advection-diffusion equation. After a number of simplifying assumptions, the pollutant concentration is computed using the Eq. (1):

$$\chi = \frac{Q}{2\pi\sigma_y\sigma_z u} e^{-\frac{y^2}{2\sigma_y{}^2}} e^{\left[\frac{-v_g(z-h)}{2K} - \frac{v_g{}^2\sigma_z{}^2}{8K^2}\right]} \left[e^{\frac{-(z-h)^2}{2\sigma_z{}^2}} + e^{\frac{-(z+h)^2}{2\sigma_z{}^2}}\right.$$
$$\left. - \sqrt{2\pi}\ \frac{v_1\sigma_z}{K} e^{\left[\frac{v_1(z+h)}{K} + \frac{v_1{}^2\sigma_z{}^2}{2K^2}\right]} erfc\left[\frac{v_1\sigma_z}{\sqrt{2}K} + \frac{z+h}{\sqrt{2}\sigma_z}\right]\right] \quad (1)$$

where χ is the pollutant concentration [g m^{-3}], K is the eddy diffusivity [m^2 s^{-1}], Q is the emission rate [g s^{-1}], u is the wind speed [m s^{-1}], σ_y, σ_z are the standard deviation of the concentration in the y and z directions [m], v_g is the gravitational settling velocity [m s^{-1}], h is the plume centerline height [m], x, y and z (height) are the coordinates of the receptor [m]. The v_1 is ($u_d - v_g/2$) where u_d is the deposition velocity [m s^{-1}], and erfc denotes the error function.

FDM incorporates point, line and area sources; the latter is used in this study. Area sources in FDM have to be rectangular up to a width to length ratio of 1–5 (Winges, 1991). In order to obtain the source input information required by the model (i.e. area sources dimensions, coordinates of the area source center point and release height of emissions), the total area of the construction site has been divided into 23 smaller area sources (Fig. 2b), formed on a grid of 50 × 50 m squares. FDM requires strictly rectangular area sources. Therefore, these squares were grouped in a way to form rectangular area sources, with different dimensions (see Fig. 2b), and to be aligned with the wind sectors. In other words, we aimed to keep each of these area sources as much as possible within the respective wind sector (Fig. 2b). Although this was not possible in all cases, it later facilitated post-processing of results and inverse calculations.

FDM expresses PM emission fluxes, owing to wind erosion, as a power function which is also supported by a large number of emission modeling studies (Sanderson et al., 2014):

$$E = Q_o u^w \quad (2)$$

where E is the emission flux [g m^{-2} s^{-1}], Q_0 is the proportionality constant [g m^{w+2} s^{1-w}], u is the wind speed [m s^{-1}], and w is the wind speed dependence factor [−]. Q_0 and w are site and soil specific parameters, respectively.

2.4. Source characterization

For the characterization of each area source, and in order to collect additional information that is necessary for FDM, we collected five soil samples (hereafter referred as SS#) from different areas of the site and conducted four different types of analysis that included bulk density calculation, particle size analysis (PSA; Beckman Coulter LS 13 320 Laser Diffraction Particle Size Analyzer, the liquid module), X-ray diffraction (XRD; Rigaku Ultima IV X-ray diffractometer) and fluorescence (XRF; Rigaku ZSX Primus II Wavelength dispersive X-ray fluorescence spectrometer). Three samples (referred to as SS1 to SS3) were collected from the

construction site area (Fig. 2b) and further two samples (i.e. SS4 and SS5) from the surrounding area, following the (USEPA, 1995) guideline for soil loading estimation. The same guideline was followed for the bulk density calculation.

The average density of the tested soil was found to be around 2340 kg m^{-3}. The crystallographic analysis showed that the soil consists mainly of 55% Dolomite ($CaMg(CO_3)_2$), 30% Calcite ($CaCO_3$), 3% Gypsum ($CaSO_4\ 2(H_2O)$) and the remaining 12% is mostly Silica (SiO_2). This is expected since the majority of the surface soil in the State of Qatar (Fig. 2a) is based on carbonates. Particle size analysis showed (Fig. 4) that most samples (SS1 to SS3) from the construction site include two modes at ~20 μm and 900 μm (particles greater than 2000 μm had been sieved out). Although the chemical and morphological compositions were similar for all samples, the samples from the surrounding area (SS4 and SS5) showed only one mode at around 900 μm. This difference is attributed to the different earthworks in the two areas. Thus, the soil of the construction site appears to have smaller particles, which would be more susceptible to Aeolian erosion. Following the above characterization and according to the Food and Agriculture Organization (FAO, 2014), this soil belongs to "Calcisols". Calcisols accommodates soils with a substantial accumulation of secondary carbonates, widespread in arid and semi-arid environments, and often associated with highly calcareous parent materials.

2.5. Evaluation of emission factors

The dispersion model, FDM, was used in an iterative manner to develop the source-receptor relationship and to calculate of the best-fitted emission flux for two averaging periods (15-min and 60-min intervals). Two to ten iterations were performed until achieving a 3 decimals accuracy (of the values reported in Table 1). The iterative calculation was performed for five particle size classes (<2.5, 2.5–6, 6–10, 10–20 and 20–30 μm) in order to match the $PM_{2.5}$ and PM_{10} fractions, and the PM fractions discussed in the AP-42; the compilation of air pollutant emission factors by USEPA (USEPA, 1995). To perform the first run of the model, the initial value for the emission flux was assumed to equal to unity and constant during the whole period. After the first iteration, the emission flux was still considered equal for all 23 rectangular shaped sources but not anymore constant for the whole modeling period. This assumption was based on the fact that the construction site surface material has uniform chemical and morphological compositions (see Section 2.4) and is exposed to the same conditions (i.e. meteorology). The model (FDM) predicted concentrations and the measured concentrations were used to correct the emission flux for each time period and size class, based on the linear relationship between the emission flux and the concentration:

$$E' = E\frac{C_M}{C_P} \tag{3}$$

where E is the emission flux [g m^{-2} s^{-1}], E' [g m^{-2} s^{-1}] is the corrected emission flux, C_p [μg m^{-3}] is the predicted concentration by the model, and C_M [μg m^{-3}] is the net measured concentration. The latter was calculated by subtracting the concentration measured by the background station from the concentration measured by the construction site station (also called receptor point as per the FDM). For the first run of FDM, E refers to the unit emission flux ($E = 1$ g m^{-2} s^{-1}).

The calculated emission fluxes (E'), for each particle size class, were classified based on the cardinal wind direction into twelve wind sectors of 30° each. The background station is positioned NNE (North-northeast; ~23°) of the construction site monitoring station, so we filtered the data and used those within the WNW to ENE (285°–75°) sectors, as shown in Fig. 2b. This wind direction range is large enough to account for all the fPM emitted from the construction site, that could reach to the receptor, and to include a representative fraction of the collected QA/QC (Quality Assured/Quality Controlled) data, in this case, ~50%. It is also small enough to consider the measurements at the background site representative of the background PM levels. Due to permission constraints, there were no other better alternative locations for the two stations. To support our assumption of the selected wind directions (WNW to ENE or 285°–75°), we examined a number of polar plots (Fig. 3b and c) for both sites. Fig. 3c shows balanced mean PM_{10} concentration levels from all wind directions for the background station, which means that no significant source affects the measurements there. For the construction site measurements (Fig. 3b), we observe mainly the impact of the construction site itself (at 285°–75°). The contribution of each wind direction and speed to the overall mean PM_{10} concentration value supports the above findings (presented as Supplementary Information, SI, Fig. S1). The correlations between the calculated emission fluxes and each of the meteorological parameters were examined in order to identify, qualitatively, the confidence in the results.

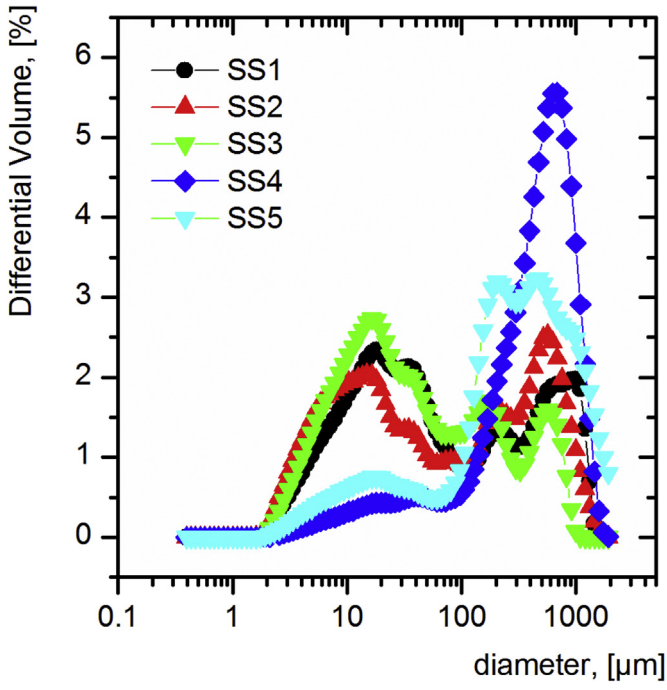

Fig. 4. Particle size analysis of the five collected soil samples (SS). Soil SS1 to SS3 are from within the construction site and SS4 and SS5 are from the nearby area.

3. Results and discussion

This section presents the results related to the fugitive emissions from the selected source. Initially, we present and discuss the actual PM measurements. Then, we discuss the correlations between the meteorology related measurements and various PM fractions. Furthermore, we present the calculated emission fluxes for each size class and compare them with literature values for similar sources (e.g. the USEPA's AP-42). Finally, we use the estimated emission fluxes to calculate the impact of the construction site, as expressed by the ground level concentrations. These concentrations are then compared with the measured data.

Table 1
Parameters of emission flux function ($E = Q_0\ u^w$; g m^{-2} s^{-1}) for four particle size class and the goodness of fit results (for hourly averages dataset).

Particle size class (μm)	Q_0	w	R^2	Adjusted R^2	RMSE[b,*]	FAC2[c,*]	FB[d,*]	NMSE[e,*]
≤2.5 ($PM_{2.5}$)	4.405×10^{-07}	1.867	0.132	0.121	0.014×10^{-5}	0.508	0.382	1.563
2.5–6	1.534×10^{-06}	1.654	0.444	0.435	1.064×10^{-5}	0.523	0.165	0.510
6–10	3.547×10^{-07}	2.691	0.693	0.688	1.272×10^{-5}	0.587	0.064	0.435
≤10 (PM_{10})	2.475×10^{-07}	2.061	0.582	0.575	2.668×10^{-5}	0.015	1.636	14.951
PM_{10} (as sum of <2.5, 2.5–6, 6–10)[a]						0.569	0.151	0.414

*Quality acceptance: FAC2>0.5 (50%); |FB| <0.3 (±30%); NMSE<0.4.
[a] Predicted emission flux based on the summation of the first three particle size classes.
[b] RMSE, Residual Mean Square Error.
[c] FAC2, Factor of Two.
[d] FB, Fractional Bias.
[e] NMSE, Normalized Mean Square Error.

3.1. Measurements

The weather during the study was typical for the period, with an average temperature of 31 ± 5 °C; there was no rainfall and average relative humidity was found to be in the range of 32 ± 22%. Prevailing wind direction was NNW (Fig. 3), which is also the annual prevailing wind direction for the region. In this work, all the measurements are averaged to 15-min and 60-min. All the data were checked manually for the purpose of quality assurance and quality control (QA/QC). For steady-state Gaussian plume models, such as FDM, periods of calm wind (i.e. wind speed <1 m s^{-1}) must be treated before entering to the model (USEPA, 2005). Data with wind speed less than 1 m s^{-1} (7.4% of the valid data) but greater than the threshold of monitoring station (i.e. 0.3 m s^{-1}) were set equal to 1 m s^{-1}, and wind speed data below the threshold of the instrument were disregarded (USEPA, 2005). We also disregarded the data for the periods when the monitoring stations were non-operational due to issues such as overheating, clogging, dust storms, and power cuts. It is worth mentioning here that there were periods where the cooling of the background station was not adequate because it was directly exposed to the sun (internal temperatures greater than 60 °C). Eventually, we used around 40% of the total data collected for the analysis and modeling purposes.

During the study period (40% QA/QC data), very high concentrations were observed at both, the construction site and background location, for all size classes. Fig. 5 presents the time series plot of the measured particulate matter (PM_{10} and $PM_{2.5}$ mass concentrations) and the wind (velocity and direction) at the site station. PM_{10} mass concentrations varied from 50 μg m^{-3} to over 600 μg m^{-3}, while $PM_{2.5}$ from 10 μg m^{-3} to 200 μg m^{-3}. Mass concentration peaks followed the high-velocity occurrences, which in turn were demonstrated mainly from northerly winds. In fact, even low wind velocities (~2 m s^{-1}) were also able to demonstrate PM_{10} concentrations of around 200 μg m^{-3}. Note that the construction site during the whole period was at rest, there were no other similar construction sites in the vicinity, and the background mass concentrations in most cases were about an order of magnitude lower than those from the construction site during the sampling period. Hence, background mass concentrations were omitted from Fig. 5.

On the other hand, during severe dust events (not included in Fig. 5) as reported by Qatar Meteorology department, the background station demonstrated concentrations of both PM_{10} and $PM_{2.5}$ about an order of magnitude higher than those at the construction site station (values were eliminated QA/QC). We could not locate a specific explanation for this trend.

3.2. Correlations between the measured concentrations and wind speeds

The correlations between all the measured data (meteorology and concentrations) for both locations and time periods were computed and investigated. The meteorological and concentration measurements at the construction site and the background location were compared in order to examine the correlation between all the variables. Concerning the 15-min averaged data, a high correlation

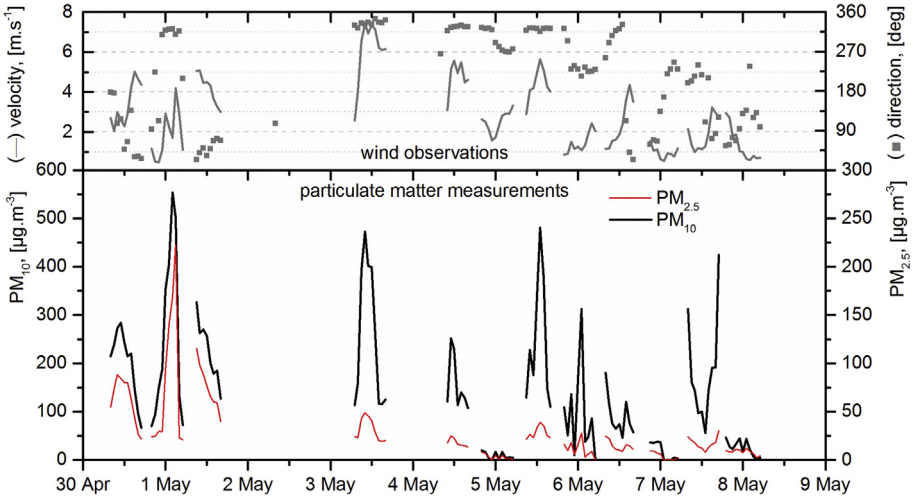

Fig. 5. A time series showing the change of mass concentration and the wind (at the construction site station) for an indicative period (~1 week) and after the exclusion of invalid data as described in Section 3.1.

(R^2 between 0.74 and 0.99) was observed between the concentrations of the different size classes at both locations. This indicates that all particle size classes are strongly related and their largest fraction is affected by the same sources. We also consider a safe assumption that the construction site produces the majority of the measured particles, based on the high difference between the concentrations at the two locations (Section 3.1). Calculation of emission fluxes was made for 15-min and hourly averages. For the 15-min averages, a correlation (R^2 between 0.32 and 0.76) was calculated between the emission fluxes and measured wind speeds at the site; the higher correlations were observed for the smaller particles' size classes (i.e. diameter ≤10 μm). This is an expected result since wind speed is the main cause of particles entrainment and favors smaller particles. It is also an indication that the origin of the majority of the smaller particles is common for the construction and background sites.

The time resolution of 15-min was initially chosen based on a rough estimate of the particles transfer time-scale from the background location to the monitoring station at the construction site. This way, it was possible to increase the number of available data points for the emission flux calculations. However, observed correlations were too low, so we used the 60-min averages (usually a standard time scale in air quality work). The obtained correlations were quite higher (i.e. R^2 between 0.34 and 0.91) and deemed satisfactory. This result can be interpreted as an effect of the distance between the two monitoring stations.

3.3. Estimation of the emission fluxes

Following the methodology described in Section 2.5, we calculated the parameters of the emission flux function (see Eq. (2)). Table 1 presents these parameters (for the hourly averages dataset) and the goodness of fit results for four particle size classes (i.e. ≤2.5, 2.5–6, 6–10 and ≤10 μm). Each function provides the developed emission flux for the corresponding particle size class and expresses the wind dependence of particles entrainment. Validation metrics (FAC2, FB, and NMSE) for the predicted emission fluxes are also provided (Table 1). Please note that PM_{10} emission flux was evaluated twice: (i) once using the predicted emission flux function, and (ii) once as a summation of the emission fluxes of the first three classes. However, as shown in Table 1, the latter case gave better results compared to the predicted function.

The goodness of fit results (Table 1) shows a better performance for larger particles, which is expected and already demonstrated by the correlations discussed in the text above. Other empirical studies have developed similar relations for the dust flux, as a power function of the wind (or friction) velocity, with parameter values of the same range as in this study. Sanderson et al. (2014) review a good number of these studies, but only a couple of them cover similar land use and soil composition. For example, Neuman et al. (2009) developed flux equations with a power factor in the range of 1.3–4 for PM_{10} for various mine tailings. Emission flux equations for total suspended particles (TSP) from different sources, including construction, was also developed by Nickling and Gillies (1989) with a power factor in the range of 1.3–3 for PM_{10} and up to 6 for TSP.

Among these studies, we selected the widely used emission inventory AP-42 (USEPA, 1995) for comparison since it is partially included in the European, Australian and other inventories. According to AP-42 the erosion potential for a dry exposed surface is calculated using the below equation:

$$P = 58(u^* - u_t^*)^2 + 25(u^* - u_t^*) \quad (4)$$

where P is the erosion potential [g m^{-2}] and u_t is the threshold friction velocity. The wind-generated particulate emissions from a surface consisting of both erodible and non-erodible material can be estimated using the below emission factor equation:

$$EF = k\sum_{i=1}^{N} P_i \quad (5)$$

where EF is the emission flux [g m^{-2} $year^{-1}$], k is the particle size multiplier, P_i is the erosion potential corresponding to the observed fastest mile of wind for the ith period between disturbances [g m^{-2}], N is the number of disturbances per year (used to adapt the Potential for the selected time scale).

AP-42 provides threshold friction velocities (from 0.43 to 1 m s^{-1}) for the selected particle sizes in the 250–4000 μm range, but not for the typical airborne particles (e.g. PM_{10} and $PM_{2.5}$). The calculated AP-42 emission rates showed very low sensitivity for threshold friction velocities less than 0.4 m s^{-1}. For simplicity, we selected a threshold value of 0 m s^{-1} Fig. 6 presents a detailed comparison of this work and the AP-42 emission fluxes. A good level of agreement is observed between this work and the AP-42. Note that the AP-42 emission fluxes were developed for open coal mines, which might demonstrate an equivalent behavior to the fine carbonated loose soil (Calcisols) of this study owing to earthworks. If one applies an apparent fitting, which is a method applied by default in many tools like Microsoft Excel, using the logarithmic expression of the power function then the resulted emission flux has a remarkably good agreement with the AP-42 ones (adjusted $R^2 > 0.90$). On the other hand, 90% prediction bands highlight the significant uncertainty of these calculations and that more studies are necessary to reduce the uncertainty and improve the accuracy (Fig. 6).

We applied the new emission fluxes to FDM for the calculation of the concentration at the receptor (construction site station) and compared them to the measured data (Fig. 7). Note that this is a plausible result because all measurements have been used for the calculation of these emission fluxes. Nevertheless, we have performed this exercise to demonstrate the overall impact of the "high" uncertainty (i.e. the 90% confidence bound in Fig. 6, indicate a high uncertainty on the estimates).

As shown in Fig. 7, modeled values (concentrations) indicate an overestimation of the net measured concentrations (note that background levels are omitted). Values are filtered in two groups based on the wind direction: (i) values within the wind sectors where emitted particles are transferred from the construction site towards the monitoring station (285°–75°), and (ii) values from the wind sectors where no emitted particles reach the monitoring station (75°–285°) from the construction site. The estimated FDM concentrations (shown in Fig. 7) are acceptable, and for PM_{10} mainly fall within the FAC2 (factor of two) statistical metric, which is a common metric in evaluating the performance of dispersion models.

4. Summary and conclusions

Air quality is progressively recognized as a critical issue for human health and is a subject for which comprehensive global emission data are missing. The release of PM from loose soils is poorly characterized in the widely used inventories and published literature. In this study, we focused on the fPM emissions from loose Calcisols (soils with a substantial accumulation of secondary carbonates) that is widely spread in arid and semi-arid environments (i.e. North Africa, Middle East, Central Asia, and Australia).

A two months field campaign was conducted at a construction

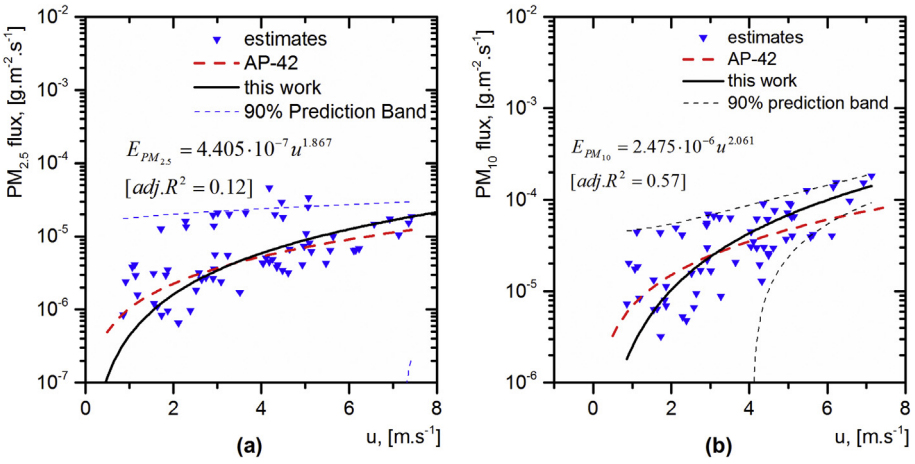

Fig. 6. Comparison between this study (estimated emission fluxes), the proposed function and AP-42 emission fluxes for (a) $PM_{2.5}$, and (b) PM_{10}. Dashed lines show the 90% confidence and prediction bands.

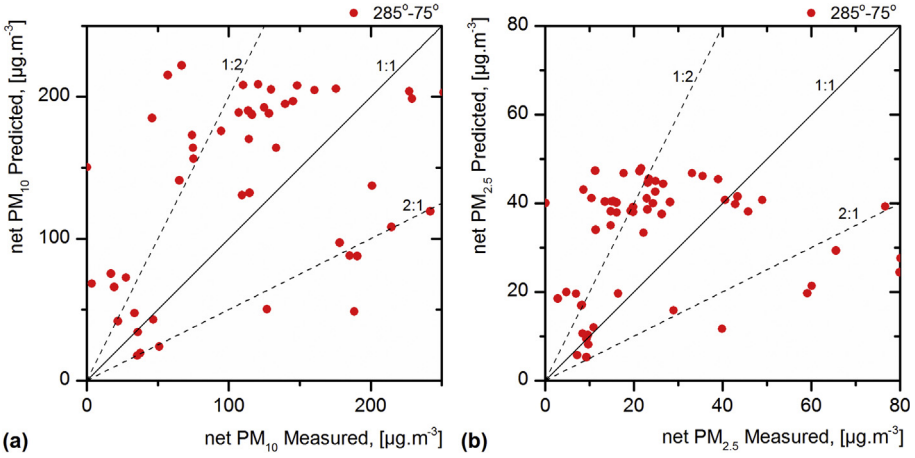

Fig. 7. Scatter plot of modeled versus measured (net) mass concentrations for: (a) PM_{10}, and (b) $PM_{2.5}$. Plots also indicate the data filtered according to wind sectors. Solid line indicates perfect agreement and dashed lines show a difference of a factor of two (FAC2).

site within the city of Doha (Qatar) to measure PM concentrations over a size range of 0.25–32 µm. The time period of the campaign was chosen deliberatively when the construction site was at rest and the only source of particles was wind erosion of the loose soil. FDM was implemented to calculate PM concentrations and obtain their emission fluxes in an iterative procedure. The model results were fitted to a power function, which expresses the wind velocity dependence. Power factors were estimated as 1.87, 1.65, 2.70 and 2.06 for the particles ≤2.5, 2.5–6, 6–10 and ≤10 µm size ranges, respectively. Power factors fitted to the data were found to show an adjusted R^2 that varied from 0.13 for the smaller particles up to 0.69 for the larger ones. These power factors are in the same range of those reported in the literature for similar sources. Other validation metrics (FAC2, FB, and NMSE) were estimated. The FAC2 results, for example, show values between 0.508 and 0.587 for almost all particle size classes. Nevertheless, and to the best of our knowledge, this is the first study focusing on construction sites (loose soil) of carbonates based soil. The loose Calcisols is potentially one of the main fPM emission sources in the Middle-East and other dry arid regions. So, the developed functions can be incorporated into particulate matter emission inventories (regional and local scale) in order to improve the assessment of health and environmental impact, and personal exposure.

On the other hand, the large uncertainty on the calculated fluxes is demonstrated by the wide 90% prediction bands, which indicates that more studies are necessary to reduce the uncertainty in estimating the fugitive emissions from similar sources. Moreover, fPM is released from a large number of other related sources (i.e. earthworks and vehicles), which are also poorly characterized. Lacking information on fPM sources is critical, given that many of these sources can be seen close to residential areas and could have a direct impact on sensitive groups such as the elderly and children. Future research should aim to demonstrate the relative impact of different (natural and anthropogenic) fPM sources in arid and semi-arid areas, their degree of dominance and eventually develop comprehensive emission inventories to fill the existing gap.

Acknowledgements

This work has been carried out under the jointly awarded grant to Texas A&M University (Qatar) and University of Surrey (UK) by the Qatar National Research Fund (a member of The Qatar Foundation; grant number: NPRP 7-649-2-241). The statements made herein are solely the responsibility of the authors.

Appendix A. Supplementary data

Supplementary data related to this article can be found at http://dx.doi.org/10.1016/j.atmosenv.2016.06.054.

References

Abdul-Wahab, S.A., 2006. Impact of fugitive dust emissions from cement plants on nearby communities. Ecol. Model. 195, 338–348.

Barlow, J., 2014. Progress in observing and modelling the urban boundary layer. Urban Clim. 10, 216–240.

Brown, K.W., Bouhamra, W., Lamoureux, D.P., Evans, J.S., Koutrakis, P., 2008. Characterization of particulate matter for three sites in Kuwait. J. Air Waste Manag. Assoc. 1995 58, 994–1003.

Bu-Olayan, A.H., Thomas, B.V., 2012. Dispersion model on PM 2.5 fugitive dust and trace metals levels in Kuwait governorates. Environ. Monit. Assess. 184, 1731–1737.

Chen, L.C., Lippmann, M., 2009. Effects of metals within ambient air particulate matter (PM) on human health. Inhal. Toxicol. 21, 1–31.

EMEP/EEA, 2013. Air Pollution Emission Inventory Guidebook. Technical report No 12/2013.

Engelbrecht, J.P., Jayanty, R.K.M., 2013. Assessing sources of airborne mineral dust and other aerosols, in Iraq. Aeolian Res. 9, 153–160.

FAO, 2014. World Reference Base for Soil Resources, World Soil Resources Reports. Food and Agriculture Organization of the UN, Rome, Italy, p. 191.

Gillette, D.A., Fryrear, D.W., Gill, T.E., Ley, T., Cahill, T.A., Gearhart, E.A., 1997. Relation of vertical flux of particles smaller than 10 μm to total aeolian horizontal mass flux at Owens Lake. J. Geophys. Res. Atmos. 102, 26,009–026,015.

Gopalaswami, N., Mannan, M.S., Kakosimos, K., Vèchot, L., Olewski, T., 2015. Analysis of meteorological parameters for dense gas dispersion using mesoscale models. J. Loss Prev. Process Ind. 35, 145–156.

Grimm, 2009. Manual, Environ Check 365. Grimm Aerosol Technik GmbH & Co, KG, Germany.

Heal, M.R., Kumar, P., Harrison, R.M., 2012. Particles, air quality, policy and health. Chem. Soc. Rev. 41, 6606–6630.

Kinsey, J.S., Linna, K.J., Squier, W.C., Muleski, G.E., Cowherd Jr., C., 2004. Characterization of the fugitive particulate emissions from construction mud/dirt carryout. J. Air Waste Manag. Assoc. 54, 1394–1404.

Kouyoumdjian, H., Saliba, N.A., 2006. Mass concentration and ion composition of coarse and fine particles in an urban area in Beirut: effect of calcium carbonate on the absorption of nitric and sulfuric acids and the depletion of chloride. Atmos. Chem. Phys. 6, 1865–1877.

Kumar, P., Morawska, L., Birmili, W., Paasonen, P., Hu, M., Kulmala, M., Harrison, R.M., Norford, L., Britter, R., 2014. Ultrafine particles in cities. Environ. Int. 66, 1–10.

Kumar, P., Pirjola, L., Ketzel, M., Harrison, R.M., 2013. Nanoparticle emissions from 11 non-vehicle exhaust sources – a review. Atmos. Environ. 67, 252–277.

Marticorena, B., Bergametti, G., 1995. Modeling the atmospheric dust cycle .1. Design of a soil-derived dust emission scheme. J. Geophys. Res. Atmos. 100, 16415–16430.

Mori, Y., 1986. Evaluation of several 'single-pass' estimators of the mean and the standard deviation of wind direction. J. Clim. Appl. Meteorol. 25, 1387–1397.

Neuman, C.M., Boulton, J.W., Sanderson, S., 2009. Wind tunnel simulation of environmental controls on fugitive dust emissions from mine tailings. Atmos. Environ. 43, 520–529.

Nickling, W.G., Gillies, J.A., 1989. Emission of fine-grained particulates from desert soils. In: Leinen, M., Sarnthein, M. (Eds.), Paleoclimatology and Paleometeorology: Modern and Past Patterns of Global Atmospheric Transport. Springer Netherlands, pp. 133–165.

Niemeyer, T.C., Gillette, D.A., Deluisi, J.J., Kim, Y.J., Niemeyer, W.F., Ley, T., Gill, T.E., Ono, D., 1999. Optical depth, size distribution and flux of dust from Owens Lake, California. Earth Surf. Process. Landforms 24, 463–479.

NPI, 1999. Emission Estimation Technique Manual for Cement Manufacturing, National Pollutant Inventory (NPI). Australian Government, Department of the Environement.

Ono, D., 2006. Application of the Gillette model for windblown dust at Owens Lake, CA. Atmos. Environ. 40, 3011–3021.

Ono, D., Kiddo, P., Howard, C., Davis, G., Richmond, K., 2011. Application of a combined measurement and modeling method to quantify windblown dust emissions from the exposed playa at Mono Lake, California. J. Air Waste Manag. Assoc. 61, 1036–1045.

Pope III, C.A., Dockery, D.W., 2006. Health effects of fine particulate air pollution: lines that connect. J. Air Waste Manag. Assoc. 56, 709–742.

Pouliot, G., Pierce, T., Denier van der Gon, H., Schaap, M., Moran, M., Nopmongcol, U., 2012. Comparing emission inventories and model-ready emission datasets between Europe and North America for the AQMEII project. Atmos. Environ. 53, 4–14.

Prabha, J., 2006. Comparison and performance evaluation of dispersion models FDM and ISCST3 for a gold mine at Goa. J. Ind. Pollut. Control 22, 297–303.

Rashki, A., Eriksson, P.G., Rautenbach, C.J.d.W., Kaskaoutis, D.G., Grote, W., Dykstra, J., 2013. Assessment of chemical and mineralogical characteristics of airborne dust in the Sistan region, Iran. Chemosphere 90, 227–236.

Roney, J.A., White, B.R., 2006. Estimating fugitive dust emission rates using an environmental boundary layer wind tunnel. Atmos. Environ. 40, 7668–7685.

Samoli, E., Peng, R., Ramsay, T., Pipikou, M., Touloumi, G., Dominici, F., Burnett, R., Cohen, A., Krewski, D., Samet, J., Katsouyanni, K., 2008. Acute effects of ambient particulate matter on mortality in Europe and North America: results from the APHENA study. Environ. Health Perspect. 116, 1480–1486.

Sanderson, R.S., Neuman, C.M., Boulton, J.W., 2014. Windblown fugitive dust emissions from smelter slag. Aeolian Res. 13, 19–29.

Schaap, M., Manders, A., Hendriks, E., Cnossen, J., Segers, A., Denier van der Gon, H., Jozwicka, M., Sauter, F., Velders, G., Matthijsen, J., PJH, B., 2009. Regional Modelling of Particulate Matter for the Netherlands. National Institute for Public Health and the Environment (RIVM), The Netherlands, p. 60.

Scott, P.K., Proctor, D., 2008. Soil suspension/dispersion modeling methods for estimating health-based soil cleanup levels of hexavalent chromium at chromite ore processing residue sites. J. Air Waste Manag. Assoc. 58, 384–403.

Shahsavani, A., Naddafi, K., Jafarzade Haghighifard, N., Mesdaghinia, A., Yunesian, M., Nabizadeh, R., Arahami, M., Sowlat, M.H., Yarahmadi, M., Saki, H., Alimohamadi, M., Nazmara, S., Motevalian, S.A., Goudarzi, G., 2012. The evaluation of PM10, PM2.5, and PM1 concentrations during the Middle Eastern Dust (MED) events in Ahvaz, Iran, from april through september 2010. J. Arid Environ. 77, 72–83.

Trivedi, R., Chakraborty, M.K., Tewary, B.K., 2009. Dust dispersion modeling using fugitive dust model at an opencast coal project of Western Coalfields Limited, India. J. Sci. Ind. Res. 68, 71–78.

Tsiouri, V., Kakosimos, K.E., Kumar, P., 2014. Concentrations, sources and exposure risks associated with particulate matter in the Middle East Area—a review. Air Qual. Atmos. Health 8, 67–80.

USEPA, 1995. Emissions Factors & AP 42, Compilation of Air Pollutant Emission Factors. U.S. Environmental Protection Agency.

USEPA, 2000. Meteorological Monitoring Guidance for Regulatory Modeling Applications. U.S. Environmental Protection Agency, Office of Air and Radiation, Office of Air Quality Planning and Standards, Research Triangle Park, NC.

USEPA, 2005. Revision to the Guideline on Air Quality Models: Adoption of a Preferred General Purpose (Flat and Complex Terrain) Dispersion Model and Other Revisions. US Environmental Protection Agency 70, pp. 68218–68261.

USEPA, 2011. Rule for Limiting Fugitive Particulate Matter Emissions, 40 CFR 49.126. United States Environmental Protection Agency.

WHO, 2005. In: Organization, W.H. (Ed.), WHO Air Quality Guidelines for Particulate Matter, Ozone, Nitrogen Dioxide and Sulfur Dioxide – Global Update 2005. http://www.who.int/phe/health_topics/outdoorair/outdoorair_aqg/en/.

WHO, 2014. Ambient (outdoor) air pollution in cities database 2014, http://www.who.int/phe/health_topics/outdoorair/databases/cities/en/.

Winges, K.D., 1991. User's Guide for the Fugitive Dust Model (FDM) Revised: User's Instructions. US Environmental Protection Agency. Report (EPA-910/9-88-202R); TRC Environmental Consultants.

Winiwarter, W., Kuhlbusch, T.A.J., Viana, M., Hitzenberger, R., 2009. Quality considerations of European PM emission inventories. Atmos. Environ. 43, 3819–3828.

Yuwono, A.S., Amaliah, L., Rochimawati, N.R., Kurniawan, A., Mulyanto, B., 2014. Determination of emission factors for soil borne dustfall and suspended particulate in ambient air. ARPN J. Eng. Appl. Sci. 9, 1417–1422.